

DVD-Quant: Data-free Video Diffusion Transformers Quantization

Zhiteng Li^{1*}, Hanxuan Li^{2*†}, Junyi Wu¹, Kai Liu¹, Linghe Kong^{1‡},
 Guihai Chen¹, Yulun Zhang^{1‡}, Xiaokang Yang¹
¹Shanghai Jiao Tong University, ²Zhejiang University

Abstract

Diffusion Transformers (DiTs) have emerged as the state-of-the-art architecture for video generation, yet their computational and memory demands hinder practical deployment. While post-training quantization (PTQ) presents a promising approach to accelerate Video DiT models, existing methods suffer from two critical limitations: (1) dependence on lengthy, computation-heavy calibration procedures, and (2) considerable performance deterioration after quantization. To address these challenges, we propose *DVD-Quant*, a novel Data-free quantization framework for Video DiTs. Our approach integrates three key innovations: (1) **Progressive Bounded Quantization (PBQ)** and (2) **Auto-scaling Rotated Quantization (ARQ)** for calibration data-free quantization error reduction, as well as (3) **δ -Guided Bit Switching (δ -GBS)** for adaptive bit-width allocation. Extensive experiments across multiple video generation benchmarks demonstrate that *DVD-Quant* achieves an approximately $2\times$ speedup over full-precision baselines on HunyuanVideo while maintaining visual fidelity. Notably, *DVD-Quant* is the first to enable W4A4 PTQ for Video DiTs without compromising video quality. Code and models will be available at <https://github.com/lhxcs/DVD-Quant>.

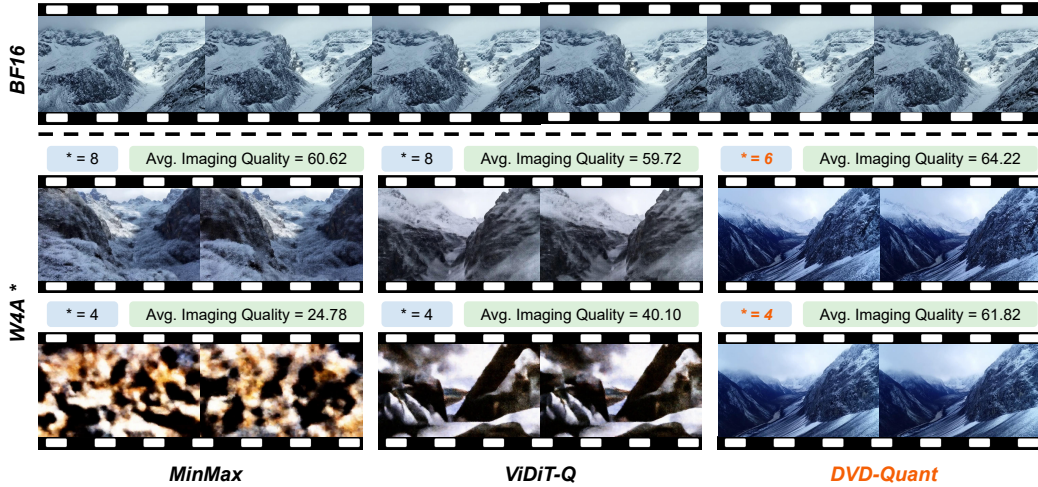


Figure 1: *DVD-Quant* generates high-fidelity videos under both W4A6 (mixed-precision) and W4A4 settings, while baseline methods fail under low-bit activation quantization. *DVD-Quant* remains effective even in such extreme scenarios.

*Equal contribution

†Work done during an internship at Shanghai Jiao Tong University

‡Corresponding authors: Yulun Zhang, yulun100@gmail.com, Linghe Kong, linghe.kong@sjtu.edu.cn

1 Introduction

Recent advances in diffusion transformers (DiTs) [28] have revolutionized video generation [32], enabling high-fidelity synthesis through iterative denoising processes. Innovations such as Sora’s unified framework [27] and SkyReels-V2’s infinite-length generation [6] demonstrate enhanced controllability, while efficiency gains emerge from quantization [42], sparse attention mechanisms [37, 41] and cache techniques [36, 21]. The emergence of large-scale models like HunyuanVideo [15] has further improved video generation quality with its causal 3D VAE architecture and full-attention mechanisms, achieving film-grade quality and physics-aware generation. These developments collectively demonstrate enhanced controllability in temporal coherence and resolution, though challenges persist in computational efficiency.

Prior work in diffusion model quantization has approached these challenges through two distinct paradigms. **Quantization-Aware Training (QAT)** requires full model fine-tuning but achieves superior low-bit performance. Ter-DiT [24] introduces RMSNorm-enhanced adaLN modules for stable ternary training of Diffusion Transformers. In contrast, **Post-Training Quantization (PTQ)** methods [17, 7, 42] offer deployment-friendly solutions without retraining. SVDQuant [17] employs low-rank SVD decomposition to absorb outliers into 16-bit branches for 4-bit weight/activation quantization on FLUX.1 models [16]. ViDiT-Q [42] introduces a set of techniques for DiT-based generative models and achieves negligible performance drop under W8A8 quantization. These approaches demonstrate the trade-off between QAT’s higher accuracy and PTQ’s faster deployment in diffusion model compression.

Despite these advances in quantization paradigms, deploying diffusion models remains challenging due to their enormous computational demands. Consider HunyuanVideo [15], one of the most advanced video generation models to date. With 13 billion parameters, applying QAT becomes impractical due to the excessive time and computational resources required for training. In contrast, PTQ provides a plug-and-play solution, but existing methods still face two critical limitations. **First**, most video-specific quantization techniques [42, 35, 7] require extensive calibration procedures, where hundreds to thousands of frames must be processed to collect activation statistics. **Second**, aggressive quantization below W4A8 (e.g., W4A4) results in significant performance degradation (Fig. 1), with VBench metrics dropping by **27.5% to 61.3%**. Our analysis reveals three key insights to overcome these limitations. (1) Weights exhibit Gaussian-like distributions (Fig. 3), making fixed quantization ranges suboptimal for preserving critical parameters. (2) Activation scales vary significantly across denoising timesteps, necessitating dynamic rather than static quantization strategies. (3) Latent feature variations exist across different denoising timesteps, enabling the possibility of adaptive bit-width allocation during online inference.

Building on these insights, we propose *DVD-Quant*, a comprehensive quantization framework featuring three key innovations. First, our **Progressive Bounded Quantization (PBQ)** employs an iterative weight quantization strategy that dynamically tightens bounds to minimize reconstruction error (Section 3.1). This approach automatically adapts to the Gaussian-like distributions characteristic of DiT weights. Second, the **Auto-scaling Rotated Quantization (ARQ)** introduces a novel activation quantization method combining Hadamard rotation with online scaling (Section 3.2). This technique eliminates calibration dependencies while controlling outliers through theoretical error bounds. Third, our **δ -Guided Bit Switching (δ -GBS)** mechanism adaptively allocates bit-widths based on feature evolution between timesteps (Section 3.3). This preserves quality during critical transformations while optimizing computational efficiency. With three techniques, *DVD-Quant* effectively addresses both weight and activation quantization challenges while preserving generation quality. Our contributions can be summarized as follows.

- A systematic analysis of quantization challenges in large-scale Video DiTs, revealing Gaussian-like weight distributions, significant activation scale differences, and latent feature variations across denoising timesteps.
- **Progressive Bounded Quantization (PBQ)**: A weight quantization technique that automatically adapts to the observed Gaussian-like distributions through dynamic bound tightening, significantly narrow down the quantization error compared to fixed-range methods.

- **Auto-scaling Rotated Quantization (ARQ):** A calibration-free activation quantization method that handles timestep-dependent scale variations through online scaling and Hadamard rotation, maintaining high accuracy without the need for extensive calibration processing.
- **δ -Guided Bit Switching:** An adaptive mixed-precision mechanism that exploits latent feature variations across timesteps to optimize bit allocation with negligible performance degradation.

2 Related Works

2.1 Diffusion Transformers (DiT)

Diffusion Transformers (DiTs) [28] represent a paradigm shift in generative modeling, replacing the traditional U-Net [8, 2, 1] backbone with transformer architectures. This breakthrough was attributed to the self-attention mechanism’s ability to model long-range dependencies [34], proving especially beneficial for high-resolution synthesis. Subsequent works like UViT [4] further refined the architecture by introducing hierarchical feature processing, leading to more efficient training and inference.

The success of DiTs in image generation quickly extended to video synthesis. Latte [26] pioneered this transition by adapting the DiT framework for temporal modeling, achieving unprecedented coherence in text-to-video generation. This was followed by Sora [27], which scaled DiTs to massive parameter counts and dataset sizes, demonstrating remarkable capabilities in long video generation with complex dynamics. Open-source implementations like HunyuanVideo [15], Open-Sora [43, 29] and CogvideoX [40] further democratized these advancements, making them widely accessible.

Despite their impressive results, DiTs inherit fundamental challenges from both transformer architectures and diffusion processes. The quadratic complexity of self-attention becomes particularly challenging for video generation, where the sequence length scales with both spatial resolution and frame count. Additionally, the iterative nature of diffusion models requires multiple forward passes through the entire architecture (typically 50-100 steps), with each step processing increasingly refined features. These limitations have spurred extensive efforts to improve DiT efficiency, including caching [36, 21], and quantization [17, 7, 42].

2.2 Model Quantization

Model quantization [38, 17, 22, 5, 18] has emerged as a fundamental technique for compressing deep neural networks by converting full-precision parameters into lower-bit representations, significantly reducing memory footprint and computational costs. Post-Training Quantization (PTQ) [19, 9, 39] has proven particularly effective as it compresses pre-trained models without requiring extensive retraining.

In transformer architectures, significant progress has been made in addressing quantization challenges. SmoothQuant [38] introduces channel-wise scaling to balance weight and activation quantization difficulty, while Quarot [3] employs orthogonal matrix rotations to distribute values evenly across channels.

For diffusion models, quantization presents unique challenges due to their time-dependent nature. Q-Diffusion [18] and PTQ4DM [31] address this by collecting timestep-wise activation statistics to determine optimal quantization parameters. The emergence of Diffusion Transformers (DiTs) has further complicated quantization, as their architectural differences from U-Net-based models require specialized approaches. Q-DiT [7] tackles channel-wise imbalance through customized quantization parameters. Subsequent work like SVDQuant [17] introduces low-rank branches to handle activation outliers, enabling 4-bit quantization without performance degradation. For video generation, ViDiT-Q [42] achieves lossless 8-bit quantization of both weights and activations.

Despite these advances, text-to-video generation with quantized DiTs still suffers from two persistent limitations. First, the huge calibration requirements of existing video quantization methods [42, 35, 7] impose impractical computational burdens, as they typically demand pro-

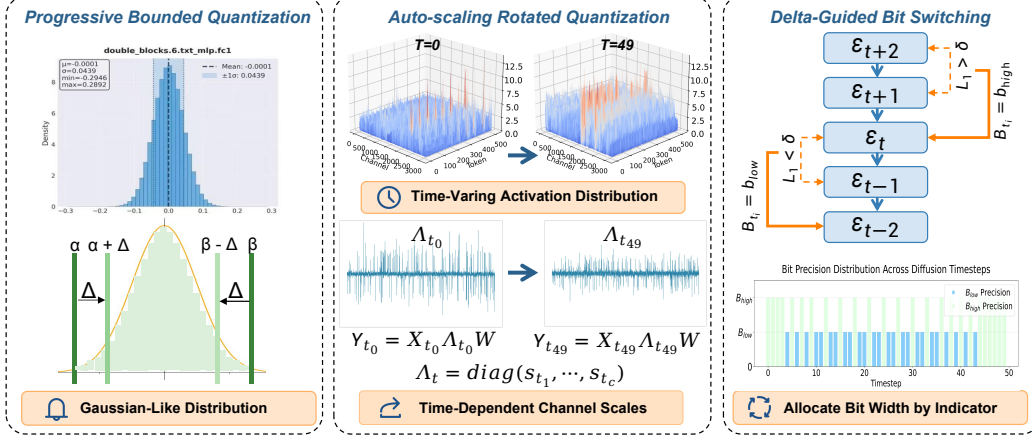


Figure 2: Overview of *DVD-Quant*. Progressive Bounded Quantization and Auto-scaling Rotated Quantization are data-free methods designed to reduce quantization errors for weights and activations, respectively. δ -Guided Bit Switching adaptively assigns bit-widths to different time steps.

cessing entire video sequences to establish activation statistics. Second, pushing quantization precision below 8 bits for activations (W4A4) triggers significant quality degradation. Our framework overcomes these obstacles through three key innovations presented in Section 3.

3 Method

Overview. As is shown in Fig. 2, Progressive Bounded Quantization (PBQ) dynamically tightens quantization bounds to preserve Gaussian-distributed DiT weights with minimal error (Sec. 3.1). Auto-scaling Rotated Quantization (ARQ) eliminates calibration overhead by jointly optimizing rotation and online scaling for activation outliers (Sec. 3.2). Together, PBQ and ARQ address weight and activation challenges. δ -Guided Bit Switching further allocates bit-widths adaptively across timesteps by tracking feature evolution. The synergy of these techniques achieves lower bit-widths (e.g., W4A4 and W4A6) with negligible quality degradation, overcoming limitations of prior quantization approaches (Sec. 3.3).

3.1 Progressive Bounded Quantization (PBQ)

The weight quantization challenge in video DiTs stems from their distinctive parameter distributions. As shown in the leftmost part of Figure 2, the weights of HunyuanVideo [15] exhibit pronounced Gaussian-like distributions centered near zero with significant long-tail effects, a pattern consistently observed across different layers. This creates two critical challenges for fixed-range quantization: (1) the min-max range becomes dominated by outlier values, wasting quantization bins on statistically insignificant parameters, and (2) the concentration of values near zero results in sparse quantization intervals in high-density regions where precision matters most.

Conventional min-max quantization directly adopts the tensor’s extreme values for range calculation through two operations: the forward quantization $Q(w) = \text{round}(\frac{w-w_{\min}}{\Delta})$ where $\Delta = (w_{\max} - w_{\min})/(2^n - 1)$ defines the step size, and the inverse dequantization $\hat{w} = Q(w) \cdot \Delta + w_{\min}$ with $w \in W$ representing the weight tensor and n the bit-width. This approach proves particularly problematic for Gaussian-distributed weights, where fixed ranges amplify quantization errors in two ways: first by allocating excessive bins to outlier regions (accounting for only 0.3% of parameters in our analysis), and second by creating suboptimal interval spacing around the zero-mean concentration.

To address this, we propose **Progressive Bounded Quantization (PBQ)** tailored for weight quantization. Inspired by [42, 22, 7], PBQ iteratively tightens the quantization boundary $\{\alpha, \beta\}$ to seek an optimal rounding error. Specifically, starting from the initial bounds $\{\alpha_0 = W_{\min}, \beta_0 = W_{\max}\}$, we progressively narrow the interval by adjusting both α

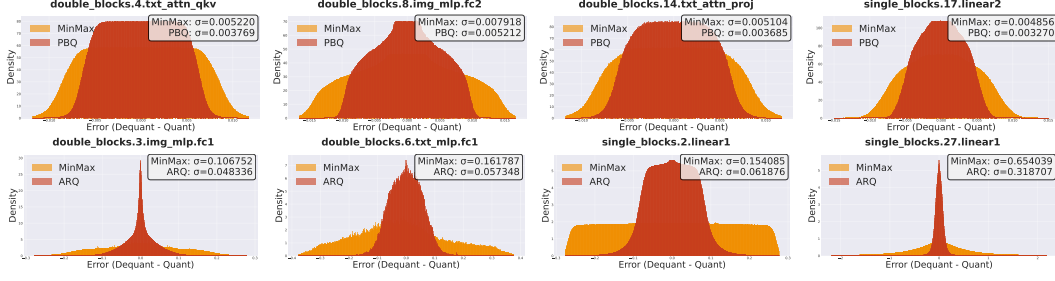


Figure 3: Quantization Error Distribution Comparison between Min-Max [12] and PBQ (top row) / ARQ (bottom row) Methods for different layers.

and β with a step size Δ :

$$\alpha_t = \alpha_{t-1} + \Delta, \beta_t = \beta_{t-1} - \Delta. \quad (1)$$

For each pair of candidates, we compute the quantized weights $Q(W)$ and evaluate the reconstruction error $\epsilon_t = \|Q(W) - W\|_2^2$. The optimal bounds are selected to minimize ϵ_t .

To further enhance robustness, PBQ operates at a per-channel granularity. For linear layers, weights are partitioned along the output channel dimension, and independent bounds are searched for each channel. By progressive bound refinement with per-channel adaptation, PBQ dynamically optimizes quantization intervals to align with intrinsic weight distributions.

Our experimental results in Figure 3 quantitatively demonstrate a substantial **39%** reduction in error standard deviation, effectively preserving the most critical parameters within high-density regions. These improvements are achieved with little computational overhead during inference, establishing PBQ as both more accurate and practically deployable compared to existing calibration-based approaches.

3.2 Auto-scaling Rotated Quantization (ARQ)

Activation quantization in Diffusion Transformers presents two fundamental challenges: **First**, the dynamic nature of activation across denoising timesteps makes offline scaling factor calibration ineffective. **Second**, traditional rotation-based approaches introduce huge online computational overhead and risk amplifying quantization errors through outlier redistribution. Existing methods fail to address these two challenges comprehensively.

Traditional scaling-based methods [38, 42, 35] introduce a per-channel mask $s \in \mathbb{R}^C$ to mitigate quantization difficulty by transferring it from activations to weights:

$$Y = (X \text{diag}(s)^{-1}) \cdot ((\text{diag}(s)W)) = \hat{X} \cdot \hat{W}, \quad s_i = \max(|X_i|)^\alpha / \max(|W_i|)^{1-\alpha}, \quad (2)$$

where α is a hyperparameter to control the extent of mitigation. Moreover, a calibration dataset is typically required to compute scaling factors offline. When applied to DiT models with 50 denoising steps [38, 42], the calibration set often fails to capture the full dynamic range of activation distributions across all timesteps, resulting in significant quantization errors. Rotation-based methods [3, 23, 42] employ an orthogonal rotation matrix Q such that $QQ^T = 1$ and $|Q| = 1$. While multiplying the matrix Q could effectively mitigate massive outliers, the rotation operation may inadvertently amplify certain activation values, potentially introducing new quantization errors in the transformed space.

To address these challenges, we propose **Auto-scaling Rotated Quantization (ARQ)** for activation quantization. Our approach combines the strengths of both rotation and scaling-based methods while overcoming their individual limitations. We first incorporate a Hadamard matrix multiplication [33] on the left and right of the activations and weights to preserve computational invariance: $Y = XW^T = (XH)(H^TW)$. Hadamard rotation is computed with the fast Hadamard transform, which introduces marginal overhead to the inference latency. After that, per-channel scaling factors are computed online and applied directly to activations rather than transferred to weights:

$$\hat{X} = Q(XH\Lambda^{-1}), \quad \hat{W} = \mathcal{P}BQ(WH), \quad Y = \hat{X}\Lambda\hat{W}^T, \quad (3)$$

where $\Lambda = \text{diag}(s_1, \dots, s_c)$, $s_j = \|\tilde{X}_j\|_\infty = \max_i |\tilde{x}_{i,j}|$.

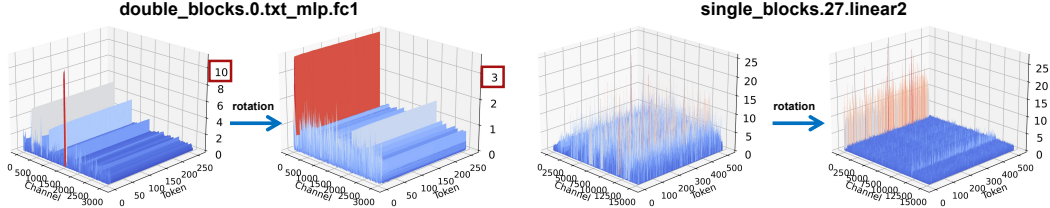


Figure 4: Visualization of activation distribution before and after rotation.

Table 1: Performance comparison of various quantization methods on VBench [11].

Method	Bit-width (W/A)	Aesthetic Quality	Imaging Quality	Overall Consist.	Scene Consist.	BG. Consist.	Subject. Consist.	Dynamic Degree	Motion Smooth.
HunyuanVideo [15]	16/16	62.53	64.78	25.86	42.81	97.01	96.05	51.39	99.30
Min-Max [12]	4/8	59.44	60.62	25.78	36.41	97.61	95.83	52.78	98.89
SmoothQuant [38]	4/8	60.50	64.47	25.56	28.85	97.72	96.29	51.39	99.05
Quarot [3]	4/8	58.80	56.86	25.33	34.30	98.10	95.72	55.56	99.03
ViDiT-Q [42]	4/8	57.01	59.74	24.77	27.11	97.37	95.16	48.61	99.06
DVD-Quant	4/6	62.27	64.22	25.83	33.07	97.89	96.57	58.33	99.05
Min-Max [12]	4/4	24.20	24.78	4.27	0.00	98.05	96.27	0.00	99.03
SmoothQuant [38]	4/4	48.41	59.46	21.09	7.84	96.72	94.97	1.39	98.79
Quarot [3]	4/4	44.85	54.30	17.33	0.94	97.69	92.64	87.5	92.22
ViDiT-Q [42]	4/4	45.36	40.10	19.66	7.85	97.19	97.29	0.00	99.43
DVD-Quant	4/4	61.96	61.82	25.68	29.94	97.82	96.61	56.94	99.15

To validate the effectiveness of our approach, we conduct an in-depth analysis of how ARQ addresses both types of outliers present in DiT activations. For channel-wise outliers, it maintains channel-wise consistency after rotation. For massive outliers, the rotation redistributes these extreme values across multiple channels, as illustrated in Figure 4, which can be processed by the per-channel smoothing mechanism. Additionally, our online scaling strategy eliminates the dependency on offline calibration datasets, which is particularly critical for DiT models where activation distributions vary significantly across the 50 denoising timesteps. This runtime adaptation ensures optimal quantization parameters regardless of the current timestep, maintaining generation quality throughout the diffusion process.

3.3 δ -Guided Bit Switching (δ -GBS)

The denoising process in video DiTs exhibits non-uniform feature evolution across timesteps. Uniform quantization wastes computational resources on these redundant timesteps while potentially compromising quality during critical transformations. Existing adaptive quantization methods either rely on expensive calibration analysis [42] or static timestep segmentation [35], unable to capture the dynamic feature w.r.t different input prompts in video generation.

To further enhance video generation quality, we introduce δ -Guided Bit Switching, tailored to the input characteristics. Previous research [14, 21, 36, 13, 25] found that denoising processes of DiT contain redundant timesteps where latent feature changes are minimal. For these steps, we can employ lower bit-width quantization across the entire model, while utilizing higher precision for critical timesteps that exhibit significant feature transformations. Specifically, our mixed-precision mechanism operates as follows:

$$B_{t_i} = \begin{cases} b_{\text{low}} & \sum_{t=t_p}^{t_i-1} \mathcal{L}_1(\mathcal{F}, t) < \delta \\ b_{\text{high}} & \sum_{t=t_p}^{t_i-1} \mathcal{L}_1(\mathcal{F}, t) \geq \delta \end{cases}, \quad \mathcal{L}_1(\mathcal{F}, t) = \frac{\|\mathcal{F}_t - \mathcal{F}_{t+1}\|_1}{\|\mathcal{F}_{t+1}\|_1}, \quad (4)$$

where t_p represents the most recent timestep where we reset our cumulative error tracking and \mathcal{F}_t denotes the model’s output features at timestep t . Our algorithm operates through continuous monitoring of normalized L1 distances between successive outputs. When cumulative feature changes remain below the threshold δ , we apply b_{low} -bit quantization, indicating minimal feature evolution that can tolerate lower precision. Once the accumulated error exceeds δ , we switch to b_{high} -bit quantization to preserve critical details, simultaneously resetting the cumulative error counter to zero. This adaptive approach ensures computational efficiency with minimal generation quality degradation. The threshold δ serves as a hyperparameter that balances performance and quality.

4 Experiments

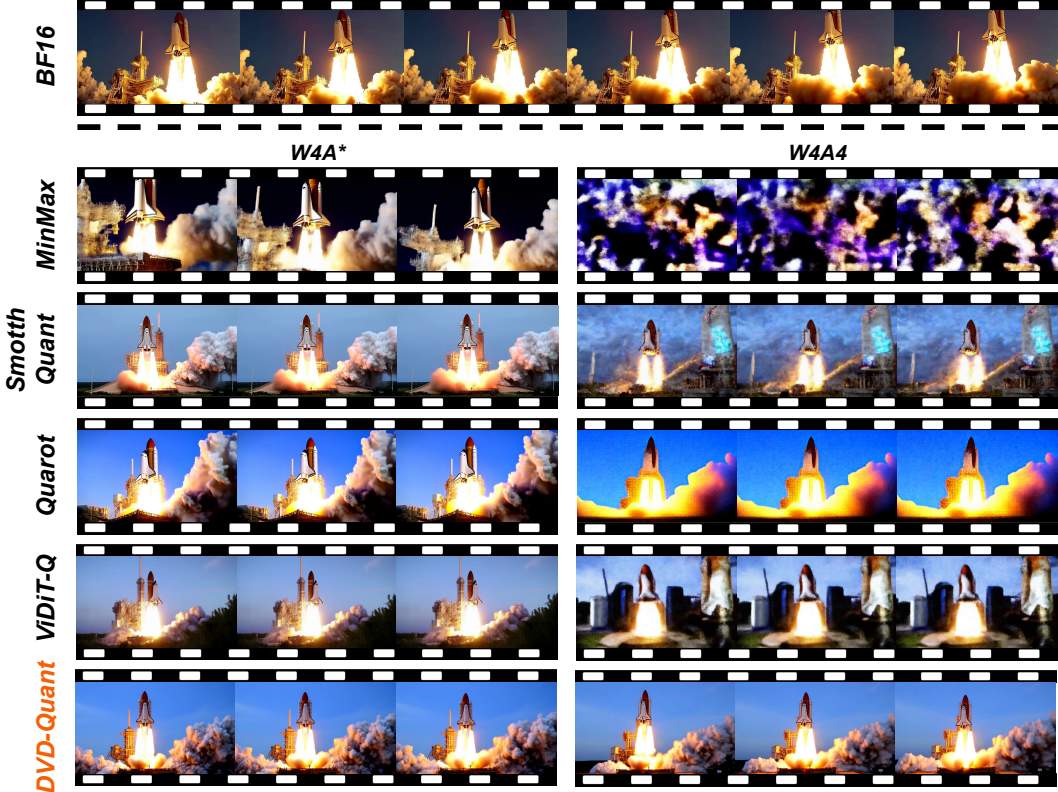


Figure 5: Visual comparisons between *DVD-Quant* and BF16 baseline [15], alongside with quantization methods: MinMax [12], SmoothQuant [38], Quarot [3] and ViDiT-Q [42]. * indicates 8 for baselines (W4A8) and 6 for *DVD-Quant* (W4A6, mixed-precision).

4.1 Setup

Video Generation Evaluation Settings: We implement *DVD-Quant* on Hunyuan-Video [15] and generate videos using a 50-step flow matching scheduler [20] with embedded CFG [10] scale 6.0 and flow shift factor 7.0. For evaluation, we adopt the benchmark suite provided by VBench [11] to comprehensively assess the quality of the generated videos. Specifically, we evaluate the model across eight major dimensions [30] that reflect key aspects of video generation. These metrics are designed to align closely with human perception, ensuring a reliable and standardized assessment of model performance. We compare *DVD-Quant* with MinMax [12], SmoothQuant [38], Quarot [3], and the current SOTA video PTQ method ViDiT-Q [42]. All experiments are conducted on a single RTX4090 GPU.

4.2 Main Results

VBench Quantitative Comparison. As shown in Table 1, *DVD-Quant* achieves significant improvements over several state-of-the-art quantization methods under two configurations. (1) **High Precision Regime:** When weights are set to 4 bits, existing methods require 8-bit activations to maintain basic functionality, while our configuration demonstrates superior performance with 25% lower activation precision. Notably, our W4A6 mixed-precision configuration nearly matches the BF16 HunyuanVideo model while significantly outperforming all W4A8 baselines across most metrics. (2) **Low Precision Challenge:** In the extremely challenging W4A4 setting where all baseline methods either fail completely or suffer severe degradation, *DVD-Quant* maintains remarkable stability. For example, we achieve 61.96 Aesthetic Quality and 61.82 Imaging Quality, closely approaching BF16 results and outperforming the best W4A4 baseline by +13.55 in Aesthetic Quality. Besides, our

method preserves temporal dynamics while maintaining high motion smoothness, whereas prior works either degrade visually or fail to generate coherent motion.

Qualitative Comparison. In W4A8 settings, while baseline methods preserve only coarse outlines, they still suffer from significant loss of fine details. As illustrated in Figure 5, ViDiT-Q’s W4A8 outputs show washed-out textures in elements like launch towers. In contrast, our method consistently recovers these subtle features, demonstrating robust performance. The advantage becomes more evident in more challenging W4A4 settings, where conventional methods fail completely, generating either incoherent noise patterns or severely distorted outputs. Our method maintains remarkable visual coherence with marginal quality degradation compared to the BF16 baseline.

4.3 Ablation Study

PBQ and ARQ. We validate the effectiveness of PBQ and ARQ in Table 3. The full model with both PBQ and ARQ achieves optimal performance across all metrics, demonstrating their synergistic effects. Removing only PBQ leads to significant drops in VBench scores, indicating the critical role of progressively narrowing the weight quantization bound to preserve perceptual fidelity. Conversely, disabling ARQ components results in comparable declines, highlighting the importance of dynamically adjusting quantization scales during inference. Both PBQ and ARQ maintain their effectiveness irrespective of δ -GBS.

Comparison with other mixed-precision strategies.

In the experiment, we set $b_{\text{low}} = 4$ bit and $b_{\text{high}} = 8$ bit in Equation (4). Our method achieves an average bit width of 6 across 50 timesteps. We compare the proposed δ -Guided Bit Switching with other fixed-pattern mixed-precision strategies. Specifically, we compare with four representative approaches: (1) **Static Temporal Partitioning (STP)**: we allocate 4-bit precision for the first 25 timesteps and 8-bit precision for the subsequent 25 timesteps; (2) **Inverse Temporal Partitioning (ITP)**: we reverse the bitwidth allocation order of STP with 8-bit initially and 4-bit later; (3) **Alternating Bitwidth Switching (ABS)**: we dynamically alternate between 4-bit and 8-bit precision at each timestep; (4) **Stochastic Bitwidth Allocation (SBA)**: we randomly assign 4-bit or 8-bit precision to each timestep while maintaining the average bit number 25. As shown in Table 2, δ -Guided Bit Switching surpasses other static mixed-precision strategies in imaging quality. This error-driven dynamic decision mechanism effectively resolves the challenge of bit allocation in conventional mixed-precision strategies.

Table 2: Performance comparison of Different mixed-precision Strategies.

Method	δ -GBS	STP	ITP	ABS	SBA
Imaging Quality	61.93	61.33	61.40	61.03	61.26

Threshold of δ -Guided Bit Switching. In our mixed-precision strategy, the threshold δ determines when to switch bit-width during inference. Empirically, a lower δ leads to more time steps using high-bit quantization, improving visual quality at the cost of increased bit-width. This presents a trade-off between performance and resource usage. Thus, we conduct a series of experiments with different thresholds. As shown in Figure 6, our experiments demonstrate that as δ increases, the average bit-width decreases, leading to a gradual reduction in imaging quality. Notably, a key advantage of δ -GBS over existing methods is its smooth and continuous bit-width adaptation: when $\delta \rightarrow 0$, the model consistently uses W4A8; when $\delta \rightarrow \infty$, it reduces to W4A4. Critically, for intermediate δ values, δ -GBS dynamically interpolates between 4-bit and 8-bit at the activation level, ensuring a continuous precision transition based on input characteristics. This smooth adaptation is in stark contrast to conventional approaches, which typically switch abruptly between discrete bit-widths, causing instability in output quality.

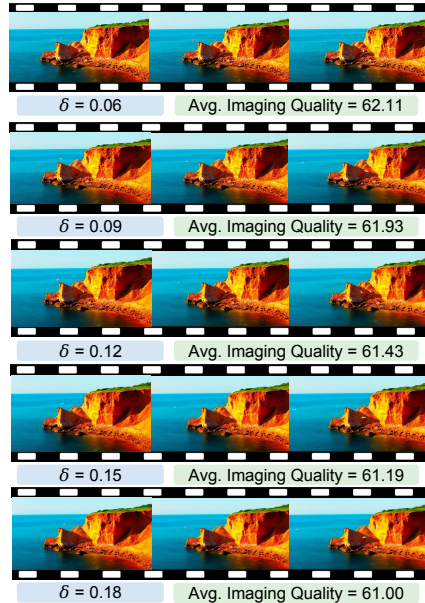


Figure 6: Illustration of visual results with different thresholds.

Table 3: Ablation studies of PBQ and ARQ under W4A6 and W4A4 quantizations.

Methods		Bit Width (W/A)	Aesthetic Quality	Imaging Quality	Subject Consist.	Motion Smooth.	BG. Consist.
PBQ	ARQ						
	✓	W4A6	58.15	58.68	98.04	98.49	98.21
✓		W4A6	57.85	57.72	98.23	97.86	98.10
✓	✓	W4A6	60.46	61.93	98.91	98.95	98.40
<hr/>							
	✓	W4A4	53.95	52.67	97.92	98.71	97.89
✓		W4A4	43.26	58.31	95.36	96.08	97.35
✓	✓	W4A4	59.57	58.93	98.67	99.00	98.47

Table 4: Performance and speedup of *DVD-Quant* + TeaCache [21].

Method	Bit-width (W/A)	Aesthetic Quality	Imaging Quality	BG. Consist.	Subject. Consist.	Motion Smooth.	Speedup
<i>DVD-Quant</i> +TeaCache	W4A8	61.39	62.96	98.24	98.73	98.75	4.01×
	W4A4	58.78	58.20	98.43	98.68	98.92	4.85×

4.4 Integrate with Cache Mechanism

To demonstrate the orthogonal compatibility of *DVD-Quant* with other compression paradigms, we conduct a systematic integration study with one of the SOTA cache methods TeaCache [21]. As illustrated in Table 4, *DVD-Quant* maintains its compression efficiency alongside TeaCache [21], achieving additive speedup (up to **4.85×**) without degrading key video generation metrics. This validates the practicality of *DVD-Quant* in resource constrained scenarios where multiple optimization dimensions could be jointly addressed.

4.5 Memory and Latency

Our quantization approach achieves significant improvements in both memory efficiency and inference speed. As shown in Table 5, compared to the BF16 baseline (16/16 bit-width), our W4A8 configuration reduces memory usage by 3.68× while accelerating latency by 1.75×. More aggressive quantization (W4A4) maintains the same memory savings but further boosts latency speedup to 2.12×. These gains stem from our innovative techniques: PBQ’s dynamic bound tightening preserves weight distributions (Sec. 3.1), while ARQ’s joint optimization handles activation outliers without calibration (Sec. 3.2). The δ -Guided Bit Switching adaptively allocates precision across timesteps, enabling mixed-precision with minimal quality loss (Sec. 3.3). Moreover, when combined with cache approaches like TeaCache, *DVD-Quant* can achieve up to 4.85× speedup.

Table 5: Memory savings and latency speedup of *DVD-Quant* compared to HunyuanVideo [15].

Bit-width (W/A)	Memory Opt.	Latency Opt.
16/16	1.00×	1.00×
4/8 (ours)	3.68×	1.75×
4/6 (ours)	3.68×	1.93×
4/4 (ours)	3.68×	2.12×

5 Conclusion

In this work, we propose *DVD-Quant*, a comprehensive quantization framework including three main innovations. The Progressive Bounded Quantization (PBQ) automatically adapts to weight distributions through iterative bound tightening, while Auto-scaling Rotated Quantization (ARQ) eliminates calibration dependencies through online rotation and scaling. The δ -Guided Bit Switching further optimizes computational efficiency through content-aware precision allocation. Extensive experiments demonstrate that *DVD-Quant* achieves 2× speedup on HunyuanVideo while maintaining visual quality, becoming the first framework to successfully enable W4A4 post-training quantization for video generation tasks.

References

- [1] Aditya Ramesh, Prafulla Dhariwal, A. N. C. C. and Chen, M. Hierarchical text-conditional image generation with clip latents. *arXiv preprint arXiv:2204.06125*, 2022.
- [2] Andreas Blattmann, Tim Dockhorn, S. K. D. M. M. K. D. L. Y. L. Z. E. V. V. A. L. e. a. Stable video diffusion: Scaling latent video diffusion models to large datasets. *arXiv preprint arXiv:2311.15127*, 2023.
- [3] Ashkboos, S., Mohtashami, A., Croci, M., Li, B., Cameron, P., Jaggi, M., Alistarh, D., Hoefler, T., and Hensman, J. Quarot: Outlier-free 4-bit inference in rotated llms. In *NeurIPS*, 2024.
- [4] Bao, F., Nie, S., Xue, K., Cao, Y., Li, C., Su, H., and Zhu, J. All are worth words: A vit backbone for diffusion models. In *CVPR*, 2023.
- [5] Benoit Jacob, Skirmantas Kligys, B. C. M. Z. M. T. A. H. H. A. and Kalenichenko., D. Quantization and training of neural networks for efficient integer-arithmetic-only inference. In *ICCV*, 2018.
- [6] Chen, G., Lin, D., Yang, J., Lin, C., Zhu, J., Fan, M., Zhang, H., Chen, S., Chen, Z., Ma, C., et al. Skyreels-v2: Infinite-length film generative model. *arXiv preprint arXiv:2504.13074*, 2025.
- [7] Chen, L., Meng, Y., Tang, C., Ma, X., Jiang, J., Wang, X., Wang, Z., and Zhu, W. Q-dit: Accurate post-training quantization for diffusion transformers. In *CVPR*, 2025.
- [8] Chitwan Saharia, William Chan, S. S. L. L. J. W. E. L. D. K. G. R. G. L. B. K. A. T. S. e. a. Photorealistic text-to-image diffusion models with deep language understanding. In *NIPS*, 2022.
- [9] Frantar, E., Ashkboos, S., Hoefler, T., and Alistarh, D. GPTQ: Accurate post-training compression for generative pretrained transformers. In *ICLR*, 2023.
- [10] Ho, J. and Salimans, T. Classifier-free diffusion guidance. *arXiv preprint arXiv:2207.12598*, 2022.
- [11] Huang, Z., He, Y., Yu, J., Zhang, F., Si, C., Jiang, Y., Zhang, Y., Wu, T., Jin, Q., Chanpaisit, N., Wang, Y., Chen, X., Wang, L., Lin, D., Qiao, Y., and Liu, Z. VBench: Comprehensive benchmark suite for video generative models. In *CVPR*, 2024.
- [12] Jacob, B., Kligys, S., Chen, B., Zhu, M., Tang, M., Howard, A., Adam, H., and Kalenichenko, D. Quantization and training of neural networks for efficient integer-arithmetic-only inference. In *CVPR*, 2018.
- [13] Junhyuk So, J. L. and Park, E. Frdiff: Feature reuse for universal training-free acceleration of diffusion models. In *ECCV*, 2024.
- [14] Kahatapitiya, K., Liu, H., He, S., Liu, D., Jia, M., Zhang, C., Ryoo, M. S., and Xie, T. Adaptive caching for faster video generation with diffusion transformers. *arXiv preprint arXiv:2411.02397*, 2024.
- [15] Kong, W., Tian, Q., Zhang, Z., Min, R., Dai, Z., Zhou, J., Xiong, J., Li, X., Wu, B., Zhang, J., et al. Hunyuanvideo: A systematic framework for large video generative models. *arXiv preprint arXiv:2412.03603*, 2024.
- [16] Labs, B. F. Flux. <https://github.com/black-forest-labs/flux>, 2024.
- [17] Li*, M., Lin*, Y., Zhang*, Z., Cai, T., Li, X., Guo, J., Xie, E., Meng, C., Zhu, J.-Y., and Han, S. Svdquant: Absorbing outliers by low-rank components for 4-bit diffusion models. In *ICLR*, 2025.
- [18] Li, X., Liu, Y., Lian, L., Yang, H., Dong, Z., Kang, D., Zhang, S., and Keutzer, K. Q-diffusion: Quantizing diffusion models. In *ICCV*, 2023.

- [19] Li, Z., Yan, X., Zhang, T., Qin, H., Xie, D., Tian, J., zhongchao shi, Kong, L., Zhang, Y., and Yang, X. Arb-llm: Alternating refined binarizations for large language models. *ICLR*, 2025.
- [20] Lipman, Y., Chen, R. T., Ben-Hamu, H., Nickel, M., and Le, M. Flow matching for generative modeling. In *ICLR*, 2023.
- [21] Liu, F., Zhang, S., Wang, X., Wei, Y., Qiu, H., Zhao, Y., Zhang, Y., Ye, Q., and Wan, F. Timestep embedding tells: It’s time to cache for video diffusion model. *arXiv preprint arXiv:2411.19108*, 2024.
- [22] Liu, K., Qin, H., Guo, Y., Yuan, X., Kong*, L., Chen, G., and Zhang, Y. 2dquant: Low-bit post-training quantization for image super-resolution. In *NeurIPS*, 2024.
- [23] Liu, Z., Zhao, C., Fedorov, I., Soran, B., Choudhary, D., Krishnamoorthi, R., Chandra, V., Tian, Y., and Blankevoort, T. Spinquant: Llm quantization with learned rotations. In *ICLR*, 2025.
- [24] Lu, X., Zhou, A., Lin, Z., Liu, Q., Xu, Y., Zhang, R., Wen, Y., Ren, S., Gao, P., Yan, J., et al. Terdit: Ternary diffusion models with transformers. *arXiv preprint arXiv:2405.14854*, 2024.
- [25] Ma, X., Fang, G., and Wang, X. Deepcache: Accelerating diffusion models for free. In *The IEEE/CVF Conference on Computer Vision and Pattern Recognition*, 2024.
- [26] Ma, X., Wang, Y., Chen, X., Jia, G., Liu, Z., Li, Y.-F., Chen, C., and Qiao, Y. Latte: Latent diffusion transformer for video generation. *TMLR*, 2025.
- [27] OpenAI. Sora: Creating video from text. *online*, 2024. Accessed: 2024-02-15.
- [28] Peebles, W. and Xie, S. Scalable diffusion models with transformers. In *ICCV*, 2023.
- [29] Peng, X., Zheng, Z., Shen, C., Young, T., Guo, X., Wang, B., Xu, H., Liu, H., Jiang, M., Li, W., Wang, Y., Ye, A., Ren, G., Ma, Q., Liang, W., Lian, X., Wu, X., Zhong, Y., Li, Z., Gong, C., Lei, G., Cheng, L., Zhang, L., Li, M., Zhang, R., Hu, S., Huang, S., Wang, X., Zhao, Y., Wang, Y., Wei, Z., and You, Y. Open-sora 2.0: Training a commercial-level video generation model in 200k. *arXiv preprint arXiv:2503.09642*, 2025.
- [30] Ren, W., Yang, H., Zhang, G., Wei, C., Du, X., Huang, S., and Chen, W. Consisti2v: Enhancing visual consistency for image-to-video generation. In *TMLR*, 2024.
- [31] Shang, Y., Yuan, Z., Xie, B., Wu, B., and Yan, Y. Post-training quantization on diffusion models. In *CVPR*, 2023.
- [32] Singer, U., Polyak, A., Hayes, T., Yin, X., An, J., Zhang, S., Hu, Q., Yang, H., Ashual, O., Gafni, O., et al. Make-a-video: Text-to-video generation without text-video data. In *ICLR*, 2023.
- [33] Tseng, A., Chee, J., Sun, Q., Kuleshov, V., and Sa, C. D. QuIP#: Even better llm quantization with hadamard incoherence and lattice codebooks. In *ICML*, 2024.
- [34] Vaswani, A., Shazeer, N., Parmar, N., Uszkoreit, J., Jones, L., Gomez, A. N., Kaiser, L., and Polosukhin, I. Attention is all you need. *arXiv preprint arXiv:1706.03762*, 2023.
- [35] Wu, J., Wang, H., Shang, Y., Shah, M., and Yan, Y. Ptq4dit: Post-training quantization for diffusion transformers. In *NeurIPS*, 2024.
- [36] Wu, J., Li, Z., Hui, Z., Zhang, Y., Kong, L., and Yang, X. Quantcache: Adaptive importance-guided quantization with hierarchical latent and layer caching for video generation. *arXiv preprint arXiv:2503.06545*, 2025.
- [37] Xi, H., Yang, S., Zhao, Y., Xu, C., Li, M., Li, X., Lin, Y., Cai, H., Zhang, J., Li, D., et al. Sparse videoen: Accelerating video diffusion transformers with spatial-temporal sparsity. *arXiv preprint arXiv:2502.01776*, 2025.

- [38] Xiao, G., Lin, J., Seznec, M., Wu, H., Demouth, J., and Han, S. SmoothQuant: Accurate and efficient post-training quantization for large language models. In *ICML*, 2023.
- [39] Yan, X., Zhang, T., Li, Z., and Zhang, Y. Progressive binarization with semi-structured pruning for llms. *arXiv preprint arXiv:2502.01705*, 2025.
- [40] Yang, Z., Teng, J., Zheng, W., Ding, M., Huang, S., Xu, J., Yang, Y., Hong, W., Zhang, X., Feng, G., et al. Cogvideox: Text-to-video diffusion models with an expert transformer. *arXiv preprint arXiv:2408.06072*, 2024.
- [41] Zhang, J., Wei, J., Zhang, P., Zhu, J., and Chen, J. Sageattention: Accurate 8-bit attention for plug-and-play inference acceleration. In *ICLR*, 2025.
- [42] Zhao, T., Fang, T., Liu, E., Rui, W., Soedarmadji, W., Li, S., Lin, Z., Dai, G., Yan, S., Yang, H., Ning, X., and Wang, Y. Vedit-q: Efficient and accurate quantization of diffusion transformers for image and video generation. *ICLR*, 2025.
- [43] Zheng, Z., Peng, X., Yang, T., Shen, C., Li, S., Liu, H., Zhou, Y., Li, T., and You, Y. Open-sora: Democratizing efficient video production for all. *arXiv preprint arXiv:2412.20404*, 2024.